

Flaw-to-grain echo enhancement by split-spectrum processing

V.L. NEWHOUSE, N.M. BILGUTAY, J. SANIIE and E.S. FURGASON

A split-spectrum processing technique for an ultrasonic flaw detection system has been developed which improves the flaw-to-grain echo ratio in large-grained materials. The enhancement is achieved by partitioning a wide-band received spectrum to obtain frequency shifted bands, which are then processed to suppress the grain echoes with respect to the flaw echo, using a novel signal minimization algorithm. Experimental data for titanium and stainless steel samples are presented which show superior flaw detection capabilities for the minimization algorithm with respect to frequency averaging techniques.

KEYWORDS: ultrasonic testing, clutter reduction, signal processing

Introduction

When the range cell of an ultrasound pulse-echo flaw detection system contains many unresolved and random reflectors such as grains, the overlapping echoes which result make the detection of flaws within the range cell difficult even when the flaws are substantially larger than the grains.

Kraus and Goebbels¹ and Kennedy and Woodmansee² have shown that the visibility of flaw echoes can be enhanced with respect to grain echoes by moving the transmit-receive transducer parallel to the flaw surface and averaging the received echoes corresponding to various transducer locations. This technique is based on the grain echo decorrelation resulting from shifts in transducer position.

There is an alternative technique which has been used in radar when targets are embedded in smaller random targets, known as clutter, which, like grains, result in unresolved and randomly distributed reflections that conceal the desired target. To improve the detection of targets in clutter, techniques known as frequency diversity or agility³⁻⁶ have been used where clutter echoes are uncorrelated by simultaneously transmitting with two or more channels centred at different frequencies or by shifting the transmitted frequency between pulses. The decorrelated received clutter signals are then averaged, which results in signal-to-clutter ratio enhancement.

It has been shown that a frequency agile system⁶ can achieve maximum clutter decorrelation when the frequency shift between the centre frequencies of successive transmitted pulses of bandwidth b obeys the relation $\Delta f \geq b$. When n such pulses of frequency spacing Δf are detected and averaged the resulting target-to-clutter power ratio will be enhanced by a factor of n or less.

Ultrasonic applications of the frequency agility concept have been limited. Koryachenko⁷ analysed the possibilities

of applying frequency agility concepts to flaw detection, while Kraus and Goebbels¹ have reported experimental results for a similar technique. In their work Kraus and Goebbels use a broad-band transducer to transmit a set of 1024 narrower-band signals, having centre frequencies randomly distributed between 3.7 and 5.3 MHz. The resulting echoes are subsequently rectified and averaged resulting in enhancement in flaw-to-grain echo ratio. The improvement in flaw visibility achieved by this procedure is of the same order of magnitude as that reported in this paper for the averaging techniques described later, but is less than that found for the minimization technique.

Techniques of this type in which one first splits a wide-band echo of bandwidth B into n bands of bandwidth B/n and then squares or rectifies and finally averages the resulting signals, cannot however be expected to provide much flaw-to-grain enhancement. This is because the first step of splitting the spectrum worsens the resolution of the resulting signals by a factor n , which consequently increases the power of uniformly distributed clutter in each range bin by n . Hence splitting the original wide-band signals into n narrower bands worsens the signal-to-clutter ratio in each of these signals by a factor n with respect to the original broad-band signal. The final averaging step then approximately restores the original flaw signal-to-grain echo ratio.

In this paper we present a different approach to flaw enhancement, referred to as split-spectrum processing, which produces frequency diverse quasi-decorrelated signals from the received wide-band signal by digital filtering instead of by transmitting many different narrow-band signals. In addition, unlike a pulse-echo system which would necessitate the use of a high speed analogue-to-digital converter, a correlation system is used whose output is at a much lower frequency than that of the transmitted signal, thus only requiring a low speed A/D converter. This system has the additional advantage of providing enhancement of the echo with respect to thermal receiver noise without the need for digital signal averaging. Finally, in order to take maximum

The authors are at the School of Electrical Engineering, Purdue University, Lafayette, Indiana, USA. Paper received 23 April 1981.

advantage of the transducer bandwidth, wide-band white noise is used as the transmitted signal.⁸ A more detailed description of these techniques is given in a later section. It should be stressed at this point, however, that the signal processing schemes described in this paper do not require the use of a random signal correlation receiver, but can be applied perfectly well to conventional pulsed rf echoes.

The last and most important aspect of the processing described in this paper is the introduction of a so-called minimization algorithm which gives results superior to the averaging procedures described above. In this technique the decorrelated or quasi-decorrelated signals are produced by splitting a wide-band echo spectrum as described above. The final enhancement signal is then produced from these signals, by plotting at each range the minimum amplitude exhibited by any of the signals at that range.

The contents of the rest of this paper are as follows. After an account of the theoretical consideration which describes the minimization algorithm we present the hardware and software aspects of the processing system. Experimental data is presented showing the dependence of the performance of the averaging and minimization algorithms on the processing parameters. Comparison of these results shows the superior flaw visibility enhancement capabilities of the minimization algorithm. Finally, additional data are presented showing the dependence of the minimization algorithm on target properties such as the grain size, angle of incidence of the sound beam on the flaw, and the flaw size.

Theory

This section reviews the considerations which led to the development of the minimization algorithm. A qualitative theory is presented which gives insight into the factors that determine the operation of this algorithm.

To analyse the operation of this algorithm we may assume that the grain boundary scatterers in the sound beam can be represented by a one-dimensional array of scatterers of cross-section A_i whose echoes reach the emitting transducer with a delay τ_i . For a correlation system illuminating a single scatterer, the output signal may be written in terms of the delay time τ as $A_i r(\tau - \tau_i)$ where $r(\tau)$ is the cross-correlation function of the transmitted signal and the echo. Hence for an array of scatterers, the correlator output amplitude as a function of delay time will be

$$u(\tau) = \sum_{i=1}^n A_i r(\tau - \tau_i) \quad (1)$$

where n is the number of scatterers contained in the range cell of the system. The width of this range cell is equal to the width of the sound beam and its length is known to be given by

$$L = \frac{c}{2B} \quad (2)$$

where c is the velocity of sound in the medium and B is the bandwidth of the transmitted signal. Hence both the length of the range cell and the number of scatterers n encompassed within it is inversely dependent on the bandwidth B .

By Fourier transforming (1), one finds the frequency dependence of the amplitude of the correlation system output signal as

$$U(f) = \sum_{i=1}^n A_i R(f - f_0) e^{-j2\pi f \tau_i} \quad (3)$$

where $R(f - f_0)$ is the Fourier transform of $r(\tau)$ and is determined by the transmitted spectrum and its centre frequency f_0 . By moving $R(f - f_0)$ outside the summation one may write (3) in the form

$$U(f) = R(f - f_0) M e^{j\theta} \quad (4)$$

where

$$M e^{j\theta} = \sum_{i=1}^n A_i e^{-j2\pi f \tau_i} \quad (5)$$

represents the phasor sum of the scatterer echoes. The power of the correlation system output signal $u(\tau)$ is proportional to $U(f) U^*(f)$ and thus to $|M|^2$.

For scatterers of constant cross-section A which are uniformly spaced within the range cell of length L one may show from (5) that the phasor magnitude can be written as,

$$\begin{aligned} |M_u| &= A \left| \frac{\sin 2\pi n \Delta x / \lambda}{\sin 2\pi \Delta x / \lambda} \right| \\ &\sim A n |\text{sinc} [2\pi L / \lambda]| \end{aligned} \quad (6)$$

for $2\pi \Delta x / \lambda \ll 1$.

Here λ is the sound wavelength, and Δx the range interval between scatterers.

$|M_u|$ is plotted as the solid line in Fig. 1, for 154 uniformly spaced, unit amplitude scatterers, and shows that the echo of such a periodic array becomes zero whenever the length L of the range cell equals an integral number of half wavelengths of the transmitted frequency, or, since L is a function of B , whenever the transmitted frequency is an integral multiple of the transmitted bandwidth, which in this case is 1 MHz. Note that the locations of the zeroes of $|M_u|$ are independent of the scatterer density L/n .

For scatterers of random cross-section that are uniformly distributed over the average cell it can be shown⁹ that

$$\langle M^2 \rangle = \{ n^2 \langle A \rangle^2 \text{sinc}^2 [2\pi L / \lambda] \} (1 - 1/n) + n \langle A^2 \rangle \quad (7)$$

where $\langle \rangle$ represents the average taken over all possible uniform distributions of the n scatterers encompassed by the range cell L . In the limit of n large and $2\pi L / n \lambda \ll 1$, (7) may be written as

$$\langle M^2 \rangle = |M_u|^2 + n \langle A^2 \rangle \quad (8)$$

which shows that on the average the power of the echo sum of randomly distributed scatterers exceeds that of uniformly spaced scatterers by the quantity $n \langle A^2 \rangle$, which is independent of frequency. $|M|$ for a sample function of 154

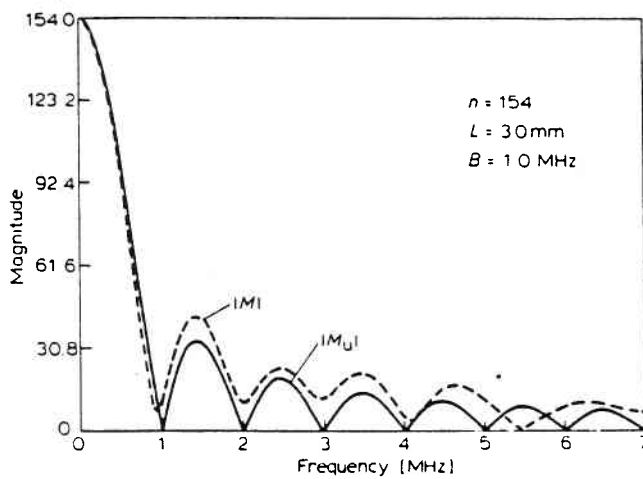


Fig. 1 Phasor magnitude against frequency for unity amplitude reflectors with: 0.02 mm uniform spacing (solid line); uniformly distributed random spacing in the 0 – 0.04 mm range (dashed line)

randomly distributed scatterers is plotted as a broken line in Fig. 1. Note that the minima in this random scatterer curve lie near those of the uniform scatterer curve, and that from (8) the average value of $|M|$ at these minima is $\sqrt{n\langle A^2 \rangle}$.

These results show that the amplitude spectrum of a random array of scatterers illuminated by a signal of bandwidth B will exhibit minima at frequencies $B, 2B, 3B$ etc, as shown in Fig. 1, provided that the number of scatterers n encompassed in the range cell of the illuminating signal is not too large. One may expect these minima to become insignificant when $\sqrt{n\langle A^2 \rangle}$ is much larger than the maxima of $|M_u|$ in the vicinity of f_0 , the centre of the transmitted spectrum. From (8) it can be shown that this occurs when

$$\sqrt{n \frac{\langle A^2 \rangle}{\langle A \rangle^2}} \gg \frac{\lambda}{2\pi\Delta x} \quad (9)$$

Using the relation $L = n\Delta x$ and substituting for L in terms of B from (2) one can rewrite (9) in the form

$$\frac{B}{f_0} \ll 2\pi^2 \frac{\Delta x}{\lambda} \frac{\langle A^2 \rangle}{\langle A \rangle^2} \quad (10)$$

This equation gives the range of values of B for which the minima in the curve of Fig. 1 should become insignificant compared to the random component.

The results derived in this section will prove useful in interpreting the experimental data presented below.

Experimental techniques

System description and data acquisition

In the work described here a wide-band transmitted noise signal centred at 5 MHz with 2 MHz half-power bandwidth is used in a random signal flaw detection system⁸ shown in Fig. 2. The electrical signals produced by the system noise source are converted to ultrasound and transmitted into the sample by the transducer. The echoes reflected from inhomogeneities are picked up by the same transducer and

correlated with the reference transmitted signal emerging from the water delay line and recorded on the x-y plotter. The correlator output resulting from a single flat-surface reflector is shown in Fig. 2b. With this system, the correlator output has been shown⁸ to result in a signal-to-thermal-noise ratio enhancement on the order of 10^4 , proportional to the product of the transmitted signal bandwidth, output low-pass filter integration time, and on-off ratio of the transmitted signal. This signal-to-thermal-noise ratio enhancement, although not related to the flaw-to-grain echo enhancement discussed in this paper, is often a useful adjunct to it in practice. A typical multiple target output of this system is shown in Fig. 3 as a function of range. The correlator output produced on the pen recorder is simultaneously sampled and relayed through an A-D converter and a microprocessor to a PDP 11/70 computer for sorting and storage. In the final step, the data stored in the PDP 11/70 computer is relayed to a CDC 6600 computer where all the data processing is accomplished.

Split-spectrum technique

In previous work the frequency averaging technique has been applied to rf flaw detection systems by shifting the centre frequency of the transmitted signal within the bandwidth of the transducer and processing the data by averaging as in radar. However, an alternative technique is possible for obtaining these individual output functions when a wide-band signal is transmitted. Thus, it can be shown that frequency-shifted signals corresponding to adjacent frequency bands can be obtained at the receiver by simply filtering the wide-band system output digitally, with equivalent results to those obtained by sequentially transmitting frequency-shifted narrow-band signals.

The split-spectrum technique described above significantly simplifies the process by which frequency-shifted signals can be obtained and subsequently processed. The computer program which splits the original wide-band output of the ultrasound correlation receiver operates as follows. The program Fourier transforms the wide-band system output to obtain the amplitude spectrum of the echo signal, divides the spectrum into the desired number of bands by means of digital filtering (see Fig. 4), and finally inverse Fourier transforms each band to obtain the individual frequency-shifted signals. The centre frequencies of these signals range within the half-power bandwidth of the transducer. The resulting signals are then normalized with respect to amplitude, giving zero-mean outputs with maximum magnitude of unity.

Fig. 5 shows sample outputs resulting from filtering the original data of Fig. 3 by means of Gaussian filters having 500 kHz bandwidth and centre frequencies at 4.64 MHz and 5.86 MHz, respectively. Note the significant variation in grain echoes resulting from the frequency shift. This strong dependence of the grain echoes on the centre frequency of the spectrum window makes flaw visibility improvement possible by processing the frequency-shifted signals using the averaging and minimization algorithms described below. In addition, the normalization of the filtered signals broadens the effective spectrum bandwidth, thus improving the system resolution.

Signal processing techniques

As mentioned previously, several techniques have been

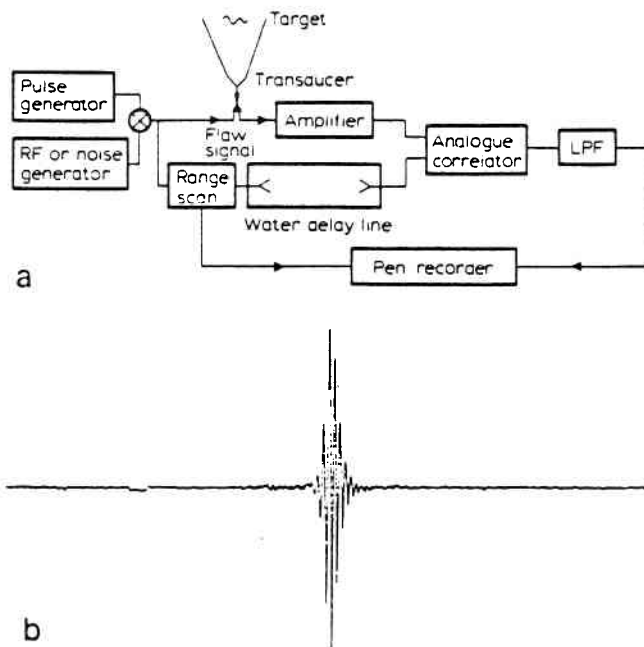


Fig. 2: a - Random signal flaw detection system with correlation type receiver; b - system output for a flat-surface reflector

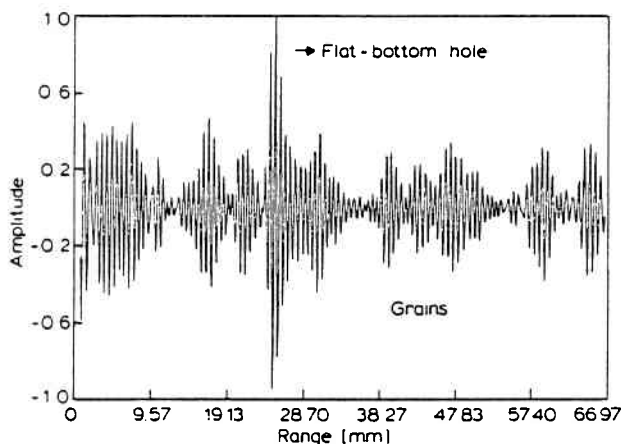


Fig. 3 Correlator output for a titanium sample with 1.19 mm diameter flat-bottom hole

employed for processing the signal set obtained from the original wide-band echo signal:

Average of squared signals

This conventional technique has been used in previous frequency averaging applications and is similar to square-law detection followed by n -pulse integration in radar. In this technique, the signals corresponding to different frequency bands are normalized, squared and then averaged. If we define $r_i(t)$ as the filtered and normalized signal corresponding to the i th band centred at frequency f_i , then the output of the averaging algorithm is given by

$$y(t) = \frac{1}{m} \sum_{i=1}^m r_i^2(t) = \bar{r}^2(t) \quad (11)$$

where m is the number of frequency-shifted signals.

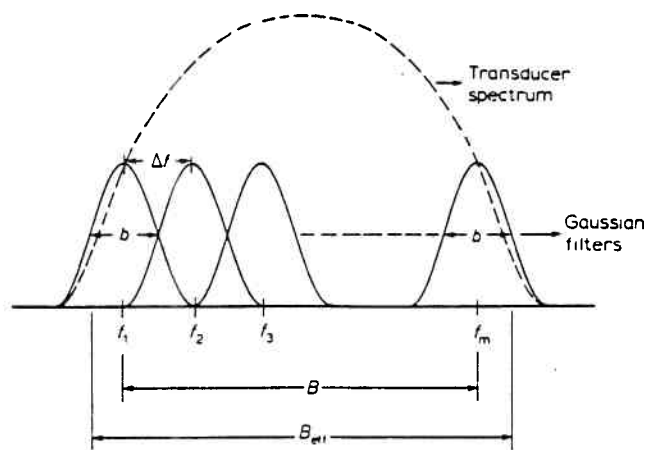


Fig. 4 Split-spectrum filtering scheme

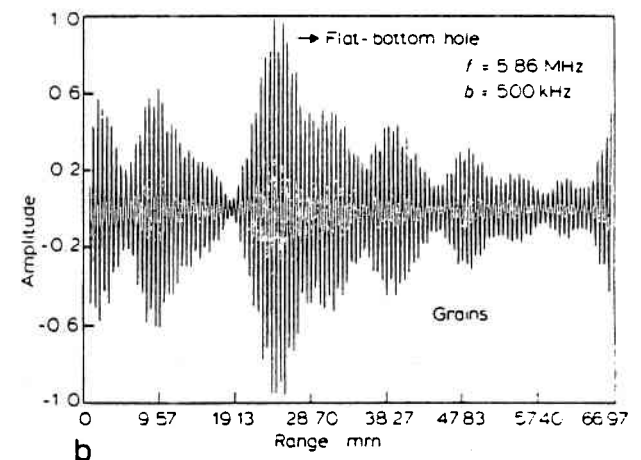
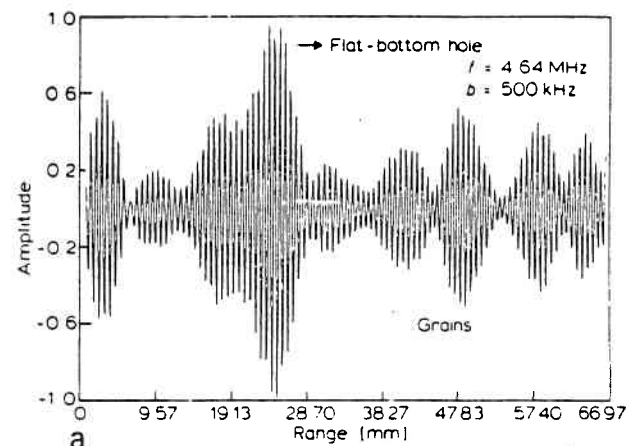


Fig. 5 Sample signals corresponding to the filtered wideband echo signal using Gaussian filters of bandwidth b and centre frequency f

Square of averaged signals

This is an alternative averaging technique which averages the normalized signals corresponding to the different frequency bands and squares the resulting signal, giving

$$y(t) = \left[\frac{1}{m} \sum_{i=1}^m r_i(t) \right]^2 = \bar{r}^2(t) \quad (12)$$

Minimization of squared signals

The minimization technique, originally introduced by this

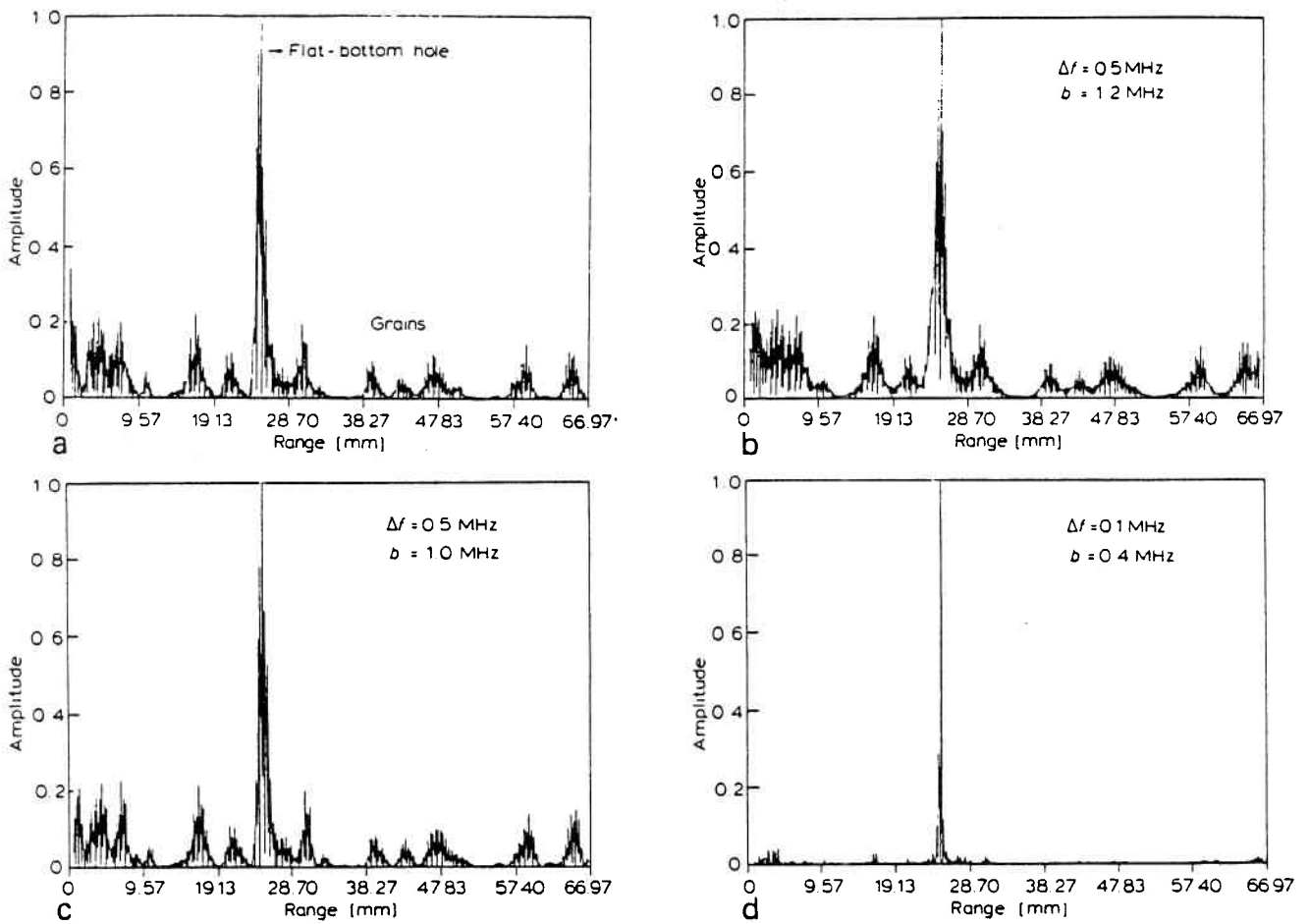


Fig. 6 Titanium data showing the squared wideband echo signal (unprocessed) and the processed outputs for the three algorithms. a — squared signal; b — average of squared signals; c — square of averaged signals; d — minimization of squared signals

indicated in Fig. 7, neither algorithm reduces the mean grain echo values with respect to those of the squared

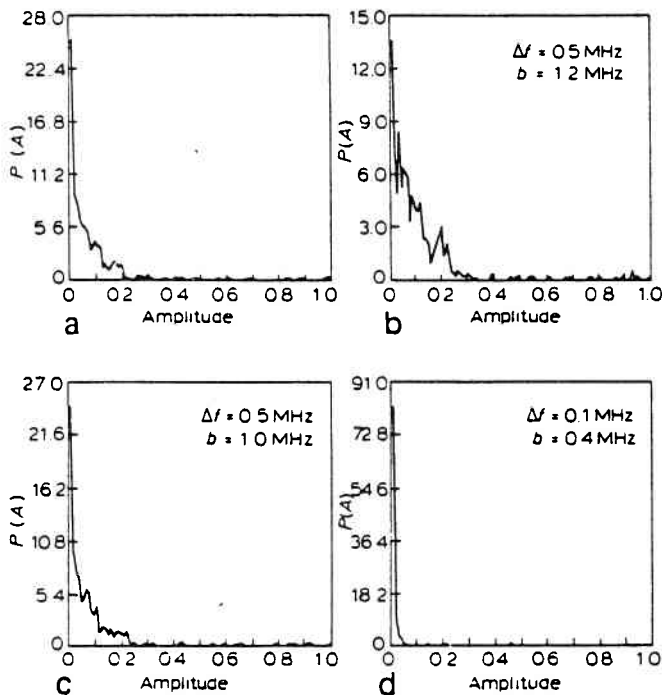


Fig. 7 Probability distribution functions corresponding to the squared wideband correlator output and the processed outputs shown in Fig. 6. a — mean 0.074, standard deviation 0.119; b — mean 0.106, standard deviation 0.142; c — mean 0.077, standard deviation 0.125; d — mean 0.013, standard deviation 0.074

wide-band signal. The 'average of squared signals' algorithm results in a higher mean value since the averaged signals are all positive and no cancellation can result between positive and negative values as in the 'square of averaged signals' algorithm. This effect becomes more pronounced for lower values of filter bandwidth b due to the reduction in resolution.

The superior performance of the minimization algorithm with respect to the averaging algorithms can be clearly seen in Figs 6 and 7. Unlike the averaging algorithms, the minimization algorithm reduces both the peak and the average grain echo values. In addition the resolution is also improved significantly, as seen in Fig. 6.

The parameter dependence of the newly introduced minimization algorithm for the titanium data is plotted in Fig. 8 as $F/G|_{\text{enh}}$ against b for various values of Δf . The results show improvement of nearly an order of magnitude in $F/G|_{\text{enh}}$ for the optimal parameters of $b = 400$ kHz and $\Delta f = 100$ kHz. It should be noted that the performance of the minimization algorithm improves with decreasing Δf , as shown by the experimental data in Fig. 8. Therefore, by optimal Δf we are referring to the saturation value in performance beyond which no significant improvement is detected. In addition to the reduction in peak grain value given by the minimization algorithm, the mean grain value also reduces significantly as can be seen in Fig. 7 by comparing the statistics of the processed data for the minimization algorithm with that of the squared signal.

It is evident that $F/G|_{\text{enh}}$ is strongly dependent on the

maximum $F/G|_{\text{enh}}$ value in Fig. 8, which occurs at a range cell on the order of 6 mm in length.

The results presented above show that for flaws simulated by flat bottom holes the split-spectrum processing technique together with the minimization algorithm is capable of significantly enhancing the flaw signal with respect to the original wide-band signal. However, the improvement obtained by the conventional averaging techniques for the same data was comparatively modest, clearly indicating the superior performance of the minimization algorithm.

In the following sections additional experimental data are presented showing the performance of the minimization algorithm under various experimental conditions resulting from the variation in material grain size, flaw amplitude, and signal incidence angle.

Flaw amplitude dependence

The effect of the input flaw-to-grain echo ratio on the performance of the minimization and averaging algorithms was studied by processing data obtained by summing previously collected grain data for stainless steel with echo data from a flat-surface reflector simulating a flaw. The particular processing parameters selected, $\Delta f = 0.1$ MHz and $b = 0.5$ MHz, are not necessarily optimal for any of the processing algorithms. However, these parameters should result in data representative of the general behaviour of each algorithm with respect to the flaw amplitude. The enhancement results were obtained for various values of input flaw-to-grain echo ratio by varying the amplitude of the simulated flaw. Fig. 9 shows the variation in the output flaw-to-maximum-grain echo ratio as a function of input

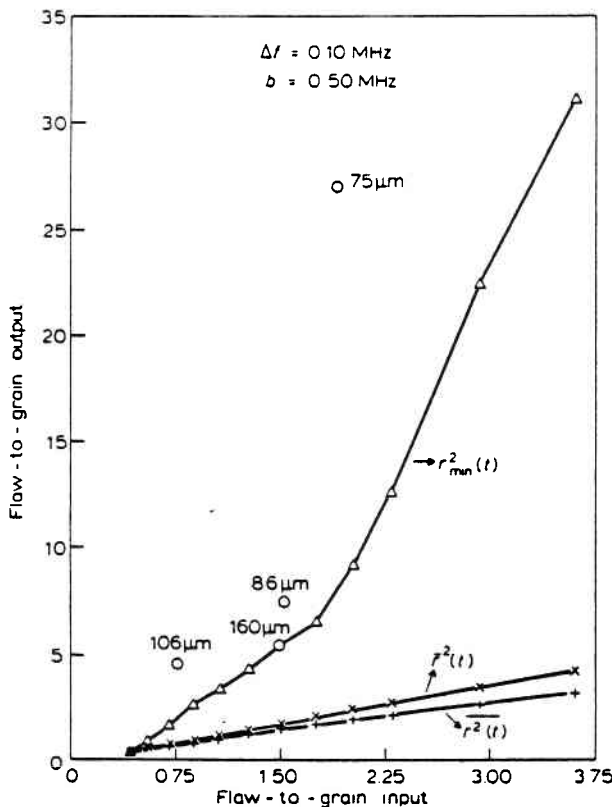


Fig. 9 Input-output flaw-to-grain echo ratio curves for the minimization and averaging algorithms from simulated flaw data in stainless steel sample of 86 μm grain size. Discrete points correspond to the optimal minimization algorithm data for flat-bottom holes in stainless steel samples of indicated grain size

flaw-to-maximum-grain echo ratio which is determined by the flat-surface reflector amplitude. (The circled numbers in Fig. 9 represent data obtained with samples of different grain sizes, which will be discussed below.)

It is clear from Fig. 9 that for both averaging algorithms the output flaw-to-grain echo ratio is linearly dependent on the input flaw-to-grain echo ratio and very little larger. These results also indicate that the 'square of averaged signal' algorithm shows slightly better performance than the 'average of squared signal' algorithm, which agrees with the previous experimental data. In addition the plots for the averaging algorithms in Fig. 9 show no noticeable enhancement in flaw-to-grain echo ratio. Since the parameters used here are not optimal, the $F/G|_{\text{enh}}$ values are somewhat less than those for the previous experimental data for which optimal enhancement values were used.

The minimization algorithm is seen to show a non-linear dependence on the input-output flaw-to-grain echo ratio, and obtains a much larger enhancement in flaw-to-grain echo ratio than the averaging algorithms, which was also demonstrated by the previous experimental data. In addition the plot indicates that the minimization algorithm achieves enhancement even when the input F/G ratio is less than unity. This means that the minimization algorithm is capable of recovering a flaw echo that is smaller than the grain echoes.*

Grain size dependence

The experimental results and theoretical considerations presented above have been primarily restricted to the case where the grain size was much smaller than the sound wavelength (Rayleigh scattering) for which multiple scattering effects can be ignored. However for a large grain environment in which the sound wavelength is on the order of the grain size (stochastic scattering) multiple scattering can no longer be neglected. Therefore multiple echoes will be received from dominant reflectors such as flaws resulting in the reduction of the effectiveness of the correlation ultrasound receiver used in the present work. It is therefore important to determine the upper limit of grain size for which our current system is effective.

To examine the performance of the split-spectrum processing under various grain size conditions, stainless steel samples consisting of large grains were prepared and tested. The desired range of grain sizes was obtained by heat treating 50.8 mm (2 inch) diameter type 304 stainless steel rods at temperatures of 1325°C, 1350°C, 1375°C and 1387°C for 1/2 - 1 h. The micrographic examination of sections taken from these samples resulted in average grain size estimates of 75, 86, 106 and 160 μm respectively, from lower to higher heat treatment temperatures. The average grain size estimates were obtained by using the linear intercept procedure. Therefore, these values actually correspond to the average grain boundary spacing, which is linearly related to the grain diameter, with the constant of proportionality determined by the grain shape. For example, this factor becomes 2.25 and 1.5 for cubic and spherical grains, respectively. However, since the grain shape is usually unknown, we prefer to define the grain size in this paper as

* The advantage of the minimization algorithm over the averaging algorithm is somewhat exaggerated in Fig. 9, since the processing parameters are nearer optimum for the minimization algorithm than for the others.

Conclusions

This paper has addressed itself to the task of detecting the presence of a single, relatively strong sound reflector (flaw) situated in the range cell of an ultrasound echo system, under circumstances where the echo from the strong reflector is dominated by the sum of echoes resulting from smaller, unresolved reflectors (grains) which fill the range cell.

Unlike the conventional frequency averaging or diversity techniques where the frequency diverse signals are generated by shifting the centre frequency of the transmitted signal within a given band, a novel technique is introduced where the echo of a broad-band transmitted ultrasound signal is split into many spectral components which are processed and subsequently recombined. Three algorithms are described which make use of the fact that echoes from scatterers too close to be resolved are dominated by interference effects such that their amplitudes vary strongly with frequency. Since the amplitudes of the echoes from the large and well-separated scatterers are affected to a lesser degree by frequency changes, a mechanism is available for extracting a large scatterer echo from the combined echo of many smaller scatterers.

Experimental data are presented that show that two of the algorithms which use conventional averaging techniques can only result in limited improvement in such systems. However, a new processing technique referred to as the minimization algorithm is shown to achieve significant improvement in flaw visibility with respect to the original wide-band output. Additional experimental data are presented showing the dependence of the minimization algorithm on various target characteristics and processing parameters.

Acknowledgements

The authors would like to thank Dr Gary Dau, our EPRI project manager, for many helpful suggestions with the research, Dr M. Behravesh of the EPRI NDE Center for providing stainless steel samples for the angle experiments, and Drs H. Kapitza and S. Kraus for a critical reading of

this paper in manuscript. We gratefully acknowledge the generous assistance of the late Dr Peter Winchell in the preparation and grain size estimation of the stainless steel samples.

This project has been supported by EPRI project number RP1395-4 and Purdue NSF-MRL Program DMR 77-23798.

References

- 1 Kraus, S., Goebels, K. Improvement of Signal-to-Noise Ratio for the Ultrasonic Testing of Coarse Grained Materials by Signal Averaging Techniques, First Int. Symp. Ultrasonic Materials Characterization, NBS, Gaithersburg, Maryland, (June 7-9, 1978)
- 2 Kennedy, J.C., Woodmansee, W.E. Signal Processing in Non-destructive Testing, *J. Testing Eval.* 3 (1) (Jan. 1975) 26-45
- 3 Gustafson, B.G., As, B.O. System Properties of Jumping Frequency Radars, *Philips Telecommunications Rev.*, 25 (1) (July 1964) 70-76
- 4 Ray, H. Improving Radar Range and Angle Detection with Frequency Agility, *Microwave J.*, (9) (May 1966) 63-68
- 5 Lind, G. Measurement of Sea Clutter Correlation with Frequency Agility and Fixed Frequency Radar, *Philips Telecommunication Rev.*, 29 (1) (April 1970) 32-38
- 6 Beasley, E.W., Ward, H.R. A Quantitative Analysis of Sea Clutter Decorrelation with Frequency Agility, *IEEE Trans. Aerospace Electronic Systems*, AES-4 (May 1968) 468-473
- 7 Koryachenko, V.D. Statistical Processing of Flaw Detector Signals to Enhance the Signal-to-Noise Ratio Associated with Structural Reverberation Noise, *Sov. J. Non-Dest. Testing*, 11 (1975) 69-75
- 8 Bilgutay, N.M., Furgason, E.S., Newhouse, V.L. Evaluation of Random Signal Correlation System for Ultrasonic Flaw Detection, *IEEE Trans. Sonics. Ultras.* SU-23 (Sept. 1976) 329-333
- 9 Beckmann, P. Statistical Distribution of the Amplitude and Phase of a Multiply Scattered Field, *J. Res. Nat. Bur. Std.*, 66D (3) (June 1962) 231-240 proves this relation for $A = 1$.
- 10 Newhouse, V.L., Furgason, E.S., Bilgutay, N.M., Saniie, J. Flaw-to-Grain Echo Enhancement, Proc. Ultras. Intern. '79, Graz, Austria. (May 1979) 152-157
- 11 Harris, J.H. On the Use of Windows for Harmonic Analysis with the Discrete Fourier Transform, *Proc IEEE*, 66 (1) (Jan. 1978) 51-83
- 12 Welch, P.D. The Use of Fast Fourier Transform for the Estimation of Power Spectra: A Method Based on Time Averaging Over Short, Modified Periodograms, *IEEE Trans. Audio Electroacoust.*, AU-15 (2) (June 1967) 70-73